Journal of Chromatography A, 1218 (2011) 408–415

Contents lists available at ScienceDirect

Journal of Chromatography A

journal homepage: www.elsevier.com/locate/chroma

Aminopropyl-functionalized ethane-bridged periodic mesoporous organosilica spheres: Preparation and application in liquid chromatography

Chun Li[a], Bin Di[a,b,*], Weiqiang Hao[c], Fang Yan[a], Mengxiang Su[a]

[a] Department of Pharmaceutical Analysis, China Pharmaceutical University, Nanjing 210009, China
[b] Key Laboratory of Drug Quality Control and Pharmacovigilance, Ministry of Education, China Pharmaceutical University, Nanjing 210009, China
[c] High-Tech Research Institute of Nanjing University, Changzhou 213164, China

ARTICLE INFO

Article history:
Received 9 September 2010
Received in revised form
16 November 2010
Accepted 22 November 2010
Available online 27 November 2010

Keywords:
Periodic mesoporous organosilicas
Aminopropyl-functionalized
Ethane-bridged
Stationary phase
Liquid chromatography

ABSTRACT

A synthetic approach for synthesizing spherical aminopropyl-functionalized ethane-bridged periodic mesoporous organosilicas (APEPMOs) is reported. The mesoporous material was prepared by a one-step co-condensation of 1,2-bis(triethoxysilyl)ethane (BTSE) and 3-aminopropyltriethoxysilane (APTES) using cetyltrimethylammonium chlorine (C_{18}TACl) as a template with the aid of a co-solvent (methanol) in basic medium. The APEPMOs were characterized by transmission electron microscopy (TEM), scanning electron microscopy (SEM), powder X-ray diffraction (XRD), nitrogen sorption measurement, Fourier transform infrared spectroscopy (FT-IR) and elemental analysis. It was shown that this material exhibited spherical morphology, ordered cubic mesostructure and good mechanical strength. The APEPMOs were tested as a potential stationary phase for liquid chromatography (LC) because the column exhibited reduced back pressure. Moreover, they exhibited good chemical stability in basic mobile phase, which can be ascribed to the ethane groups in the mesoporous framework.

1. Introduction

Since the discovery of periodic mesoporous organosilicas (PMOs) in 1999 [1], these novel materials have attracted significant attention in the fields of adsorption and separation [2,3]. PMOs have the advantages of mesoporous silicas such as high surface area and narrow pore size distribution. However, they have other unique properties including enhanced hydrothermal and mechanical stability. Recently, PMOs have been identified as a promising stationary phase for liquid chromatography [4].

In recent years, aminopropyl-functionalized PMOs have been synthesized for various applications such as base-catalysis [5], chemical reactions [6], absorption [7] and bio-separation [8]. Zhang et al. synthesized amino-functionalized mesoporous ethane-silicas with highly ordered 2D mesopores using a template of Pluronic P123 ($EO_{20}PO_{70}EO_{20}$) and an inorganic additive (KCl) in acidic medium [5]. Among these studies, the factors affecting the formation of uniform mesopores have been extensively investigated. However, less attention has been given to the control of the external appearance of the mesoporous materials. Generally, spherical morphology is requested for the packing materials for LC to obtain high column efficiency. Thus far, there are still only a few reports on the preparation of spherical aminopropyl-functionalized PMOs.

The earliest literature describing spherical PMOs was reported by Rebbin, who synthesized the ethane-silica spheres by the modified Stöber method [9]. To date, there have been many reports on the synthesis of spherical mono-functionalized PMOs, such as ethane-bridged [10–13] and phenylene-bridged PMOs [14–16]. Compared to the mono-functionalized PMOs, the multi-functionalized PMOs are anticipated to provide enhanced separation due to the combination of several retention mechanisms. Zhu et al. synthesized a series of bifunctionalized PMOs for LC [17–19]. These phenyl-functionalized ethane-bridge organosilicas exhibited better separation of polycyclic aromatic hydrocarbons than C_8-immobilized mesoporous silicas [17]. The chiral PMOs that were synthesized by incorporating *trans*-(1*R*,2*R*)-diaminocyclohexane into the organosilica framework showed higher enantioselectivity of nine amino acids over other chiral silica stationary phases [18]. The chiral PMOs with *trans*-(1*R*,2*R*)-bis-(ureido)-cyclohexane bridged in the organosilica framework provided baseline separation of (*R*/*S*)-1,1′-bi-2-naphthol enantiomers at high sample loading and high flow rate [19].

In the present study, spherical aminopropyl-functionalized PMOs with a particle size range of 3–8 μm were synthesized for the first time by co-condensation of 1,2-bis(triethoxysilyl)ethane (BTSE) and 3-aminopropyltriethoxysilane (APTES). This meso-

* Corresponding author at: Department of Pharmaceutical Analysis, China Pharmaceutical University, Nanjing 210009, China. Tel.: +86 25 83271269; fax: +86 25 83271269.
E-mail address: ddw888@vip.sina.com (B. Di).

0021-9673/$ – see front matter © 2010 Elsevier B.V. All rights reserved.
doi:10.1016/j.chroma.2010.11.048

porous material was bifunctionalized, meaning that it contained both aminopropyl and ethane functional groups. The functional groups were introduced into the material during a one-step co-condensation process. Compared to the traditional methods for the synthesis of stationary phases such as grafting, coating and immobilization, the present method can provide an facile way o synthesize the stationary phase with uniformly distributed organic groups. The aminopropyl-functionalized ethane-bridged periodic mesoporous organosilicas (APEPMOs) were demonstrated as potential new packing materials for LC columns.

2. Experimental

2.1. Chemicals and materials

3-Aminopropyltriethoxysilane (APTES, 99%) and 1,2-bis(triethoxysilyl)ethane (BTSE, 96%) were purchased from J&K Chemicals (Nanjing, China) and Sigma–Aldrich Company Ltd. (USA), respectively. Octadecyltrimethylammonium chloride (C_{18}TACl) was purchased from Sinopharm Chemical Reagent Corporation (Shanghai, China). Stainless-steel tubes (250 mm × 4.6 mm I.D.) and a Lichrospher NH_2 column (250 mm × 4.6 mm I.D.; pore diameter, 10 nm; particle size, 5 μm) were purchased from Hanbon Technologies (China). A Thermo APS-2 HYPERSIL NH_2 column (250 mm × 4.6 mm I.D.; pore diameter, 12 nm; particle size, 5 μm) was purchased from Thermo. Methanol, ethanol, isopropanol and *n*-hexane were HPLC-grade and purchased from Tedia (USA). Deionized water was produced on a PureLab Classic (DI, UK) water purification system. Other chemicals were commercially available and used as received.

2.2. Preparation of APEPMOs

In a typical synthesis of APEPMOs-3, the template (1.47 g C_{18}TACl) was dissolved in a solution containing water (28.8 mL) and methanol (22.8 mL), followed by the addition of 0.66 M NaOH (17.0 mL) and a mixture of BTSE (1.44 mL) and APTES (0.66 mL). After stirring at room temperature for 3 h, the solution was transferred into a Teflon-lined autoclave and heated at 90 °C for 16 h. The white precipitate was recovered by filtration, washed with deionized water and dried at 100 °C. The molar ratios for the synthesis of different APEPMOs (denoted as APEPMOs-*n*, *n* = 0–4) are listed in Table 1. The surfactants in the materials were extracted by stirring 1.0 g of as-synthesized material in 150 mL ethanol containing 3 mL of 36 wt.% HCl aqueous solution for 5 h at room temperature. After filtration, the sample was washed thoroughly with ethanol and dried at 100 °C. This process was repeated one time.

2.3. Characterization methods

FT-IR spectra were taken on a Spectrum Nicolet 6700 FT-IR spectrometer (Thermo, USA) with smart diffuse reflectance. X-ray powder diffraction (XRD) patterns were recorded on a Thermo ARL X-ray diffractometer (USA) using Cu Kα radiation (λ = 1.54 Å). Diffraction data were collected from 0.5° to 8° (2Theta) with a resolution of 0.01° at a voltage of 40 kV. The nitrogen sorption experiments were performed at 77 K in the relative pressure range of 0.0–1.0 on a Micromeritics ASAP 2020M surface areas and porosity analyzer (USA). The samples were outgassed at 100 °C for 10 h before the measurement. The surface area was estimated using the Brunauer–Emmett–Teller (BET) method. The pore size distribution was calculated from the desorption branch of the isotherm using the Density Functional Theory (DFT) method. Transmission electron microscopy (TEM) was collected using a JEM-200CX (JEOL, Japan) at an acceleration voltage of 80 kV. Scanning electron microscopy (SEM) images were realized on a Hitachi S-3400N microscope (Japan). The samples were deposited on a sample holder with an adhesive carbon foil and sputtered with gold prior to imaging. Elemental analysis was performed on an Elementar Vario ELIII (Germany). The particle size distribution was carried out in a MasterSizer S particle size analyzer (Malvern, UK).

Table 1
Molar ratios for the synthesis of APEPMOs.

Sample	APTES	BTSE	C_{18}TACl	NaOH	Methanol	H_2O
APEPMOs-0	0	1	0.6	1.6	80	360
APEPMOs-1	0.1	0.9	0.6	1.6	80	360
APEPMOs-2	0.25	0.75	0.6	1.6	80	360
APEPMOs-3	0.4	0.6	0.6	1.6	80	360
APEPMOs-4	0.5	0.5	0.6	1.6	80	360

2.4. Chromatographic tests

2.4.1. Apparatus and operating conditions

LC separations were carried out using a Shimadzu LC-20AT prominence HPLC system (Japan) consisting of a vacuum degasser, a quaternary pump, a Rheodyne 7725i injector with a 20 μL injection loop and a SPD-20A detector. The response from the detector was recorded by HS2000 data analysis software (Hangzhou Empire Science & Techn. Co., Ltd., China). The chromatographic columns were packed with the synthesized materials into a 250 mm × 4.6 mm I.D. stainless steel tube using the slurry technique. Prior to packing, the stainless steel tube was passivated with $CHCl_3$ and 0.1 mol/L HNO_3, followed by a thorough washing with deionized water and methanol. The packing materials were dispersed in ethanol and packed into the column under 50 MPa with the same solvent. The column was enclosed with end fittings and washed with methanol for 12 h before use. The samples were solved in the mobile phase and the concentrations of them were 5 μg/mL. The injection volume was 20 μL. The column temperature was kept at 25 °C. Each separation was repeated in triple.

2.4.2. Column aging procedure

Alkaline column degradation studies were performed as follows [20]: in this procedure, columns were challenged with a 50 mM triethylamine (TEA) solution (pH 10.0) in water for 120 min (2.0 mL/min, 25 °C) and then purged with water (2.0 mL/min, 25 °C) and methanol (2.0 mL/min, 25 °C) for 10 min each. After that, they were purging with water (2.0 mL/min, 25 °C) and methanol (2.0 mL/min, 25 °C) for 20 min each. The efficiency of the columns was then tested using a mixture of uracil (used to define the dead time) and anthracene as solute and a methanol/H_2O mixture (50/50, v/v, 25 °C) as the mobile phase at the flow rate of 1.0 mL/min with UV detection at 254 nm.

3. Results and discussion

3.1. Morphology control of the APEPMOs

The morphology of the mesoporous materials obtained under different synthesis conditions was investigated using the SEM technique (Fig. 1). It was found that the APEPMOs synthesized in the presence of both surfactant (C_{18}TACl) and co-solvent (methanol) exhibited well-formed spherical morphology with a particle size range of 3–8 μm (Fig. 1b–d). The SEM image of the sample synthesized without methanol is shown in Fig. 1a. This material contains massive broken pieces, indicating that the co-solvent (methanol) plays an important role in the formation of spherical morphology. The addition of alcohols during the synthesis may decrease the polarity of the solvent and retard the hydrolysis rates of the organosilane precursors. The slow assembly of the hydrolyzed

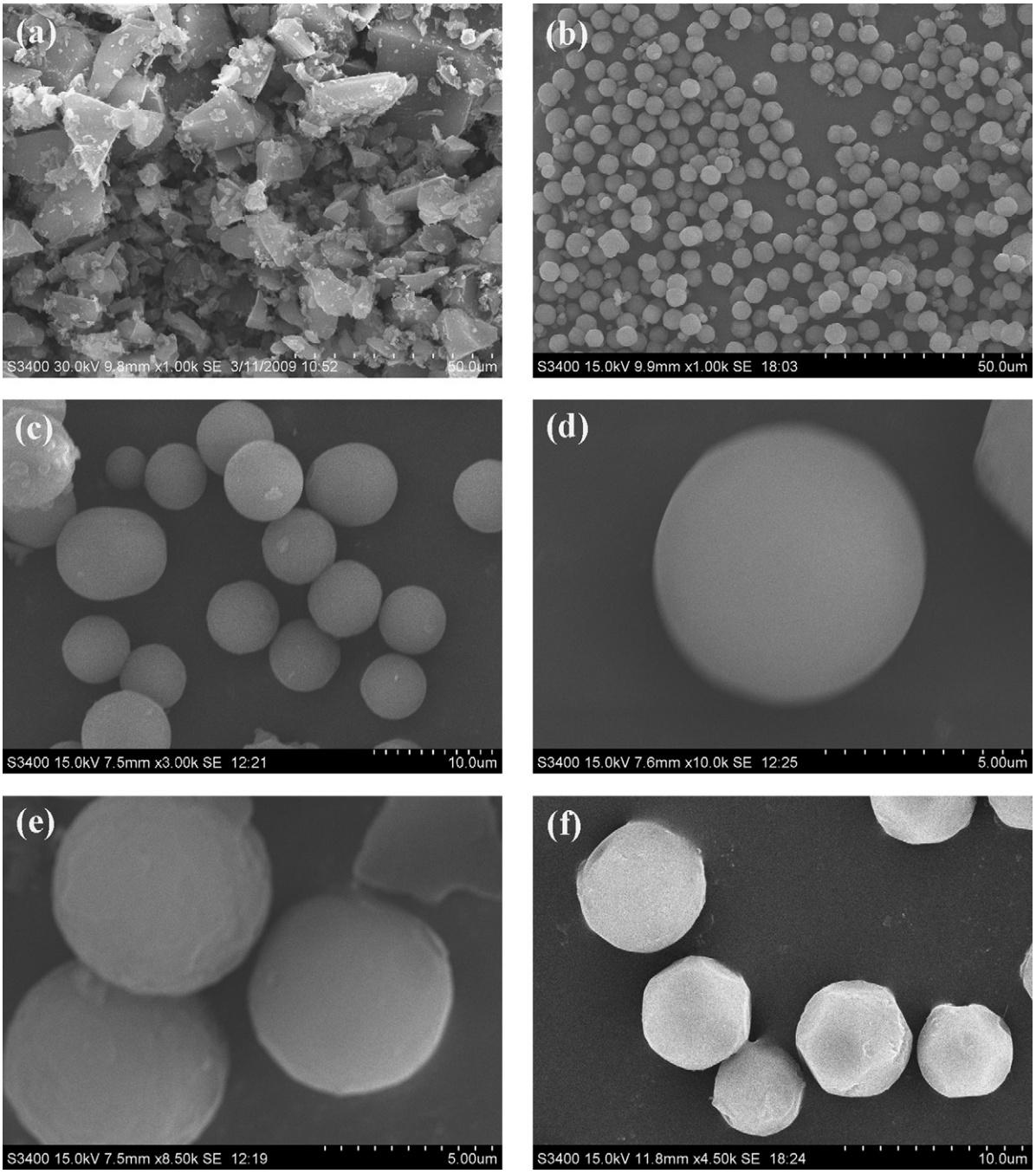

Fig. 1. SEM images of extracted APEPMOs: (a) APEPMOs-3 (synthesized without adding methanol); (b–d) APEPMOs-3 (molar ratio of APTES:BTSE = 0.4:0.6); (e) APEPMOs-4 (molar ratio of APTES:BTSE = 0.5:0.5) and (f) APEPMOs-3 (synthesized at the aging temperature of 120 °C). Other synthesis conditions were the same as those in Section 2.2.

silane species around the surfactant micelles can contribute to the formation of organosilica spheres [17]. Ethanol was also used as co-solvent. The spherical morphology was obtained, but the production rate was somewhat lower than that of methanol. Therefore, methanol was selected as the co-solvent in the present study.

Experimentally, it was determined that the spherical morphology of APEPMOs could be maintained when the molar ratio of APTES/BTSE was varied from 0.1:0.9 to 0.5:0.5. By increasing the molar ratio of APTES in the reaction solution, high NH_2 loading capability was obtained. However, this caused the surface of the spheres to become rough (Fig. 1e). By controlling both the NH_2 loading capability and smooth surface of the particles, the molar ratio of APTES/BTSE = 0.4:0.6 provided the most desirable results.

The effects of aging temperature and aging time on the morphology of mesoporous materials were also investigated. The aging temperature was varied from 70 to 140 °C and the aging time varied from 10 to 24 h. The SEM image of representative APEPMOs-3 synthesized at the aging temperature of 120 °C is shown in Fig. 1f, and the particle size distribution (Fig. 2) proves that almost microspheres is among 3–8 μm, with average of 5.9 μm. The morphology of the material synthesized at the high aging temperature changed to a multi-faced decaoctahedral shape. It was also established that a high aging temperature and short aging time led to a small particle size. After several trials, a 90 °C aging temperature and a 16 h aging time were selected for the synthesis of spherical APEPMOs with a particle size of approximately 5 μm.

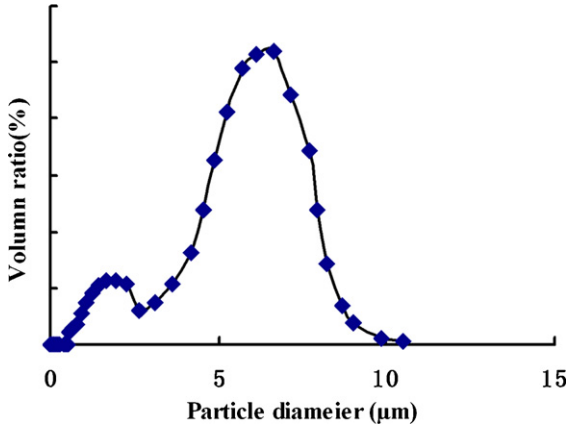

Fig. 2. The particle size distribution of APEPMOs-3.

To investigate the mechanical stability of the synthesized organosilicas, APEPMOs-3 were packed into a stainless-steel column under 50 MPa and washed with a methanol/H_2O mixture (50/50, v/v) at 1.0 mL/min for 24 h. The packing material was removed from the column, and the SEM images that collected before and after packing are displayed in Fig. 3. It is evident that the spheres maintain the same morphology and particle size even after high-pressure packing and long-term solvent washing. This result demonstrates the robust morphological properties of the synthesized APEPMOs.

3.2. Mesostructure of the APEPMOs

The textural properties of representative APEPMOs-3 are summarized in Table 2. XRD patterns of extracted APEPMOs-0, APEPMOs-2 and APEPMOs-3 are shown in Fig. 4. The intense (2 1 0) diffraction peak around 2° indicates that all of these materials have highly ordered mesopore. APEPMOs-0 (synthesized in the presence of only BTSE) exhibits only the (2 1 0) peak. When APTES is introduced into the synthetic process, the (2 1 1) peak appears next to the (2 1 0) peak, indicating that APEPMOs-2 and APEPMOs-3 have a cubic *Pm*3*n* phase [21]. With increasing NH_2 loading density (from APEPMOs-0 to APEPMOs-3), the intensity of the (2 1 0) and (2 1 1) peaks is decreased, indicating that the pore structure became less ordered. High quantities of aminopropyl groups would occupy the pore space and may be the main reason for the less ordered mesostructure [5,18]. The pore wall thickness of APEPMOs-3 is about 1.51 nm, calculated by subtracting the pore-diameter from the lattice unit parameter. The uniform pore wall thickness will help to form a stronger framework to improve overall mechanical stability of the material.

Nitrogen sorption isotherm and corresponding pore size distribution of extracted APEPMOs-3 are illustrated in Fig. 5. The sample exhibits type IV isotherm with a sharp capillary condensation step in the medium range of the relative pressure, which reflects a highly uniform mesopore arrangement [22]. This result is also confirmed by the TEM image shown in Fig. 6. The pore diameter was in the range of 3–5 nm, with average of 4.09 nm. The pore volume was

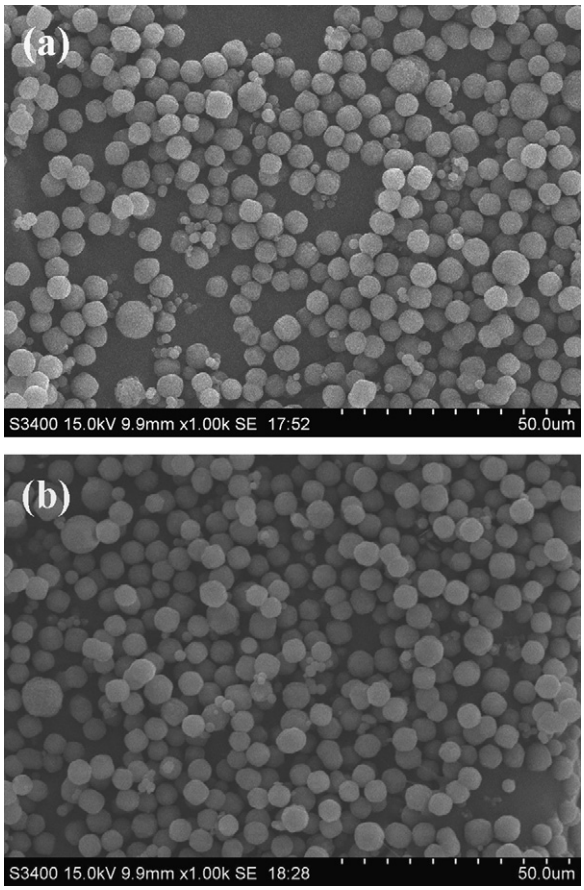

Fig. 3. SEM images of APEPMOs-3 (a) before and (b) after packing.

calculated to be 0.585 cm^3/g, and other physical parameters listed in Table 2. The BET-specific surface area was calculated as 765 m^2/g, which is roughly 2 times higher than that of most commercial packing materials (300–450 m^2/g) [20]. This result demonstrates that the synthesized material has a high specific surface area.

3.3. Compositional characterization of the APEPMOs

To clarify the preservation of the organic functional groups in the mesoporous materials, FT-IR and elemental analysis measurements were conducted. Fig. 7 illustrates the FT-IR spectra of representative APEPMOs that were synthesized according to the molar ratios listed in Table 1. These spectra display similar band profiles.

The large broad band between 3200 and 3700 cm^{-1}, one of the main features of the spectrum, is referred to the N–H bond stretching of aminopropyl groups and O–H one of the surface silanol groups. The bands between 2890 and 2930 cm^{-1} are attributed to C–H stretching of aminopropyl and ethane groups. C–H bending vibrations were also observed at 1416 cm^{-1} [5]. The band around 1470 cm^{-1} illustrates the NH_2 stretching vibration. The band at 1200 cm^{-1} is ascribed to the C–N stretching vibration, whereas the band at 1631 cm^{-1} is attributed to asymmetric vibration of

Table 2
Textural parameters of APEPMOs-3.

S_{BET} (m^2/g)	Pore size[a] (nm)	Pore volume (cm^3/g)	*d*-Spacing[b] (nm)	a_0[c] (nm)	Pore wall thickness[d] (nm)
765	4.09	0.585	4.85	5.60	1.51

[a] Calculated from desorption branch using DFT method.
[b] Calculated by small angle XRD (d-spacing = $\lambda/2 \sin\theta$).
[c] Unit cell parameter ($a_0 = 2d$-spacing/31/2).
[d] Calculated by subtracting the pore size from a_0.

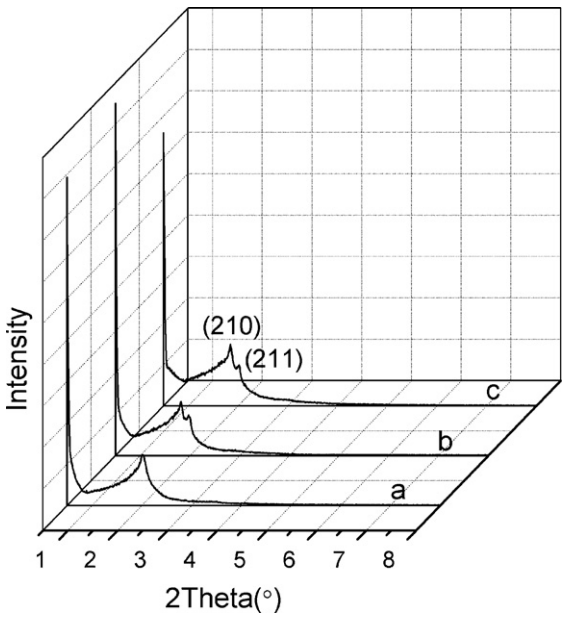

Fig. 4. XRD patterns of extracted APEPMOs: (a) APEPMOs-0; (b) APEPMOs-2 and (c) APEPMOs-3.

N–H. Peaks around 1100 cm^{-1} indicates the existence of the siloxane, –Si–O–Si–, and Si–O bond stretching of silanol groups was observed as a small band at 990–945 cm^{-1}. These results support the existence of aminopropyl and ethane groups in the mesoporous materials. Fig. 8 shows FT-IR spectra of representative APEPMOs-3 before and after surfactant extraction. The intensity of the bands assigned to the surfactant C_{18}TACl (2922 and 2855 cm^{-1} [23]) is greatly reduced in the FT-IR spectrum of extracted sample APEPMOs-3. This result indicates that most of the surfactant was removed by the solvent extraction method.

Elemental analysis results are presented in Table 3. With increasing molar composition of APTES in the reaction solution, the amino group content in the materials is increased. Accordingly, the content of ethane groups is decreased but still is maintained at a high level (~6.4 mmol/g).

3.4. LC tests

The APEPMOs-3 with spherical morphology (3–8 μm) was slurry-packed into a LC column. The operating pressure for this column was compared to the commercial NH_2 column (Lichrospher) (Fig. 9). To compare with different NH_2 column, a Thermo APS-2 HYPERSIL NH_2 column (250 mm × 4.6 mm I.D., 12 nm, 5 μm) was newly purchased to test the pressure. Under the same conditions, the pressure for the APEPMOs-3 column is about one-half of that in the NH_2 column. Permeability (K) and dimensionless flow resistance parameter (ϕ) are calculated according to the following

Table 3
Elemental analysis results for APEPMOs.

Sample	Element content (wt.%)		Organic group loading (mmol/g)	
	C	N	NH_2[a]	$-CH_2CH_2-$[b]
APEPMOs-1	16.44	0.14	0.10	6.70
APEPMOs-2	16.29	0.20	0.14	6.57
APEPMOs-3	16.58	0.45	0.32	6.43
APEPMOs-4	17.30	0.74	0.53	6.42

[a] Calculated from N content.
[b] Calculated from the remaining C content that was obtained by subtracting the C content in aminopropyl groups from that in total.

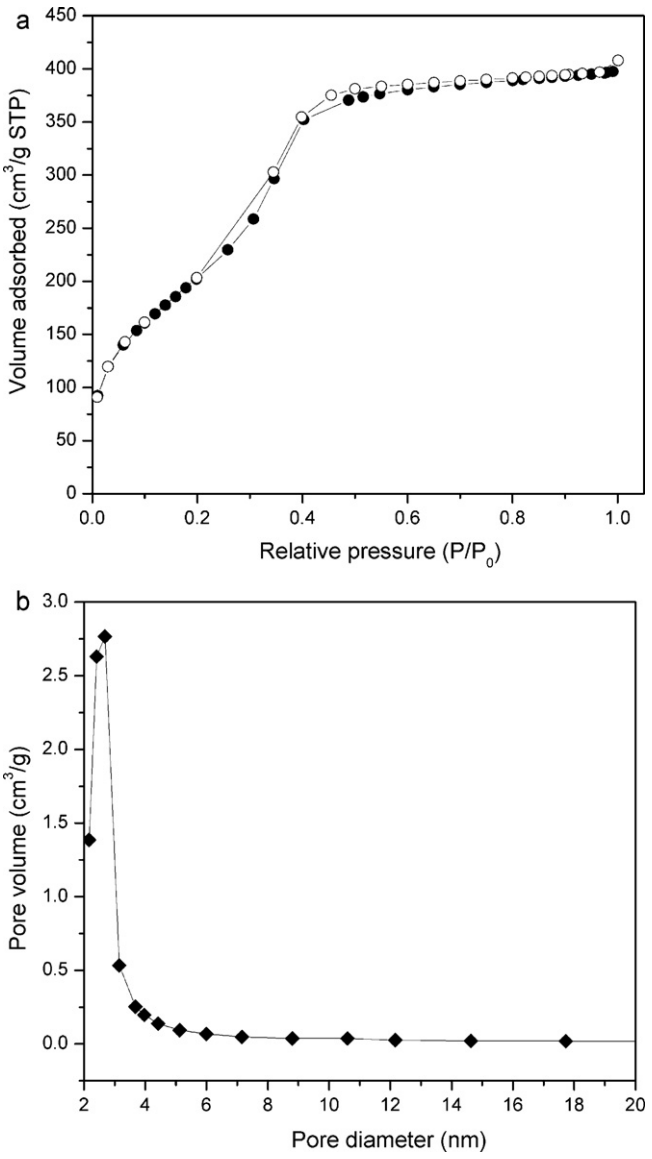

Fig. 5. (a) Nitrogen adsorption (close)–desorption (open) isotherm and (b) pore size distribution of extracted APEPMOs-3.

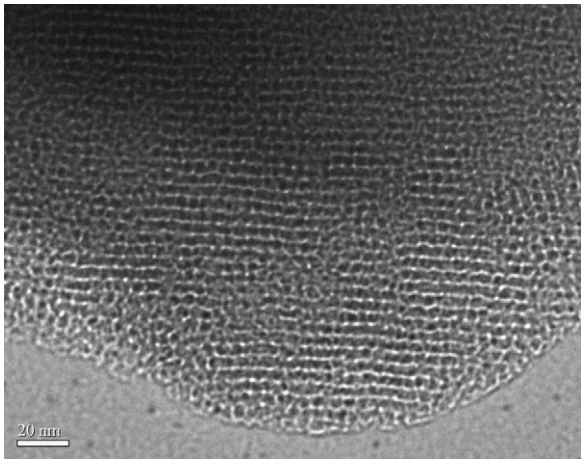

Fig. 6. TEM image of extracted APEPMOs-3.

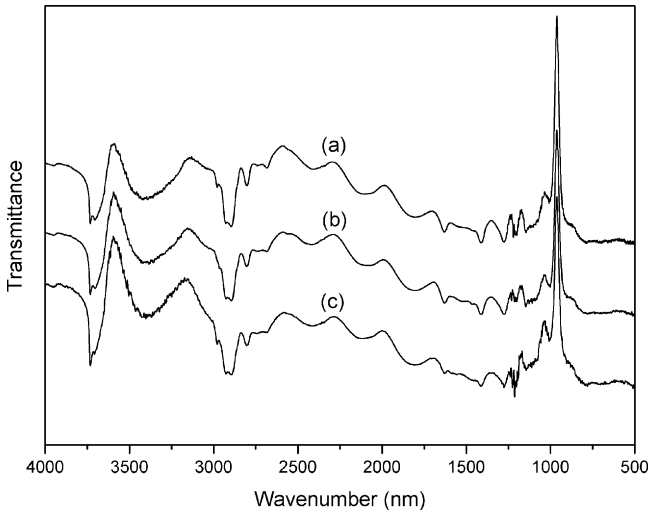

Fig. 7. FT-IR spectra of extracted APEPMOs: (a) APEPMOs-0; (b) APEPMOs-2 and (c) APEPMOs-3.

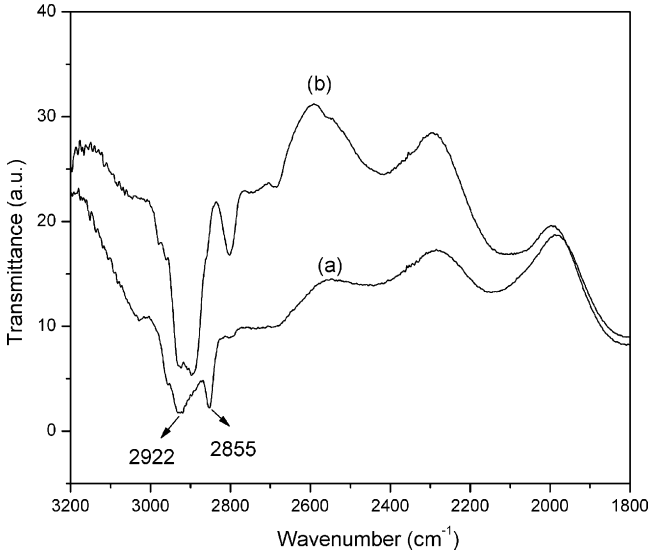

Fig. 8. FT-IR spectra of APEPMOs-3 (a) before and (b) after surfactant extraction.

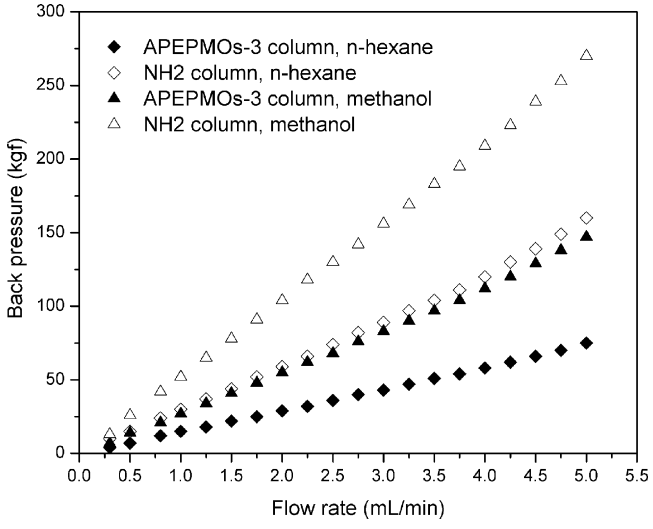

Fig. 9. Comparison of the pressure/flow behavior between the APEPMOs-3 and commercial NH_2 columns (250 mm × 4.6 mm I.D., 5 μm). Mobile phase: *n*-hexane and methanol.

Table 4
Permeability and flow resistance parameter of the APEPMOs-3 and commercial NH_2 columns.

Column	Eluent	K ($\times 10^{-14}$ m^2)[a]	ϕ[b]
APEPMOs-3	Hexane	6.87	364
APS-2 HYPERSIL NH_2	Hexane	3.65	685
APEPMOs-3	Methanol	6.94	360
APS-2 HYPERSIL NH_2	Methanol	3.83	653

[a] Permeability, calculated by Eq. (1).
[b] Permeability, calculated by Eq. (2).

equations [24]:

$$K = \frac{u\eta L}{\Delta P} \quad (1)$$

$$\phi = \frac{d_p^2}{K} \quad (2)$$

where u is the linear velocity of eluent, η the dynamic viscosity of eluent, L the column length, ΔP the pressure drop. The values of these parameters, which were calculated by using the experimental results obtained at flow rate of 1.0 mL/min, are presented in Table 4. It can be seen that the APEPMOs-3 column has much better permeability and lower flow resistance that the commercial NH_2 column. The above results can be attributed to the highly ordered mesostructure of APEPMOs-3. The low operating pressure will be beneficial to the maintenance of the LC pumps. Moreover, this low-backpressure advantage makes it possible to reduce the analysis time by increasing the flow rate. Fig. 9 shows the chromatograms for the separation of benzene derivatives (toluene, biphenyldimethylesterate and nitrobenzene) on the APEPMOs-3 column at different flow rates. Base-line separation can be achieved within 4 min. At this flow rate of 4.0 mL/min, the operating pressure is only about 42 kgf. In addition, the peaks in Fig. 10 appear to be somewhat broad. This broadness is primarily due to the non-uniform interspaces among the packing materials because the particle size obtained is not uniform. Further work is underway to synthesize APEPMOs with a more uniform particle size.

Some kinds of compounds were selected to test on our as-prepared column using high pH mobile phase. It is found that in extremely basical (pH 11.8) condition, the APEPMOs-3 column had good performance on the separation of metronidazole, fluconazole and isonicotinic acid (Fig. 11). What's more, some

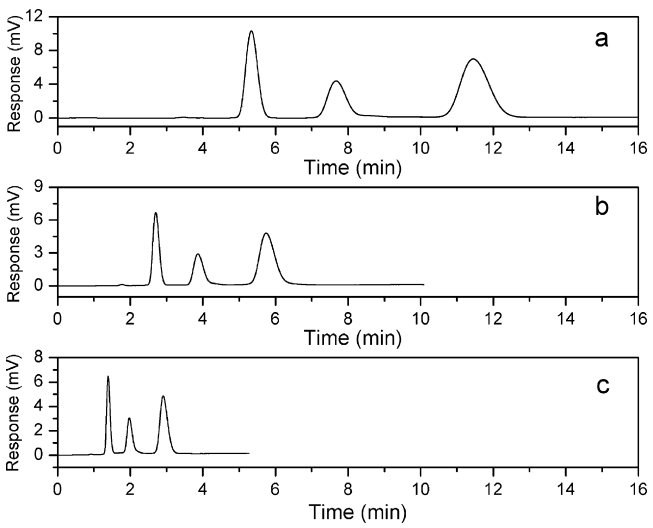

Fig. 10. Separation of benzene derivatives on the APEPMOs-3 column at flow rate of (a) 1.0 mL/min; (b) 2.0 mL/min and (c) 4.0 mL/min. Mobile phase: *n*-hexane. UV: 254 nm. Peaks from left to right: toluene, biphenyldimethylesterate, nitrobenzene.

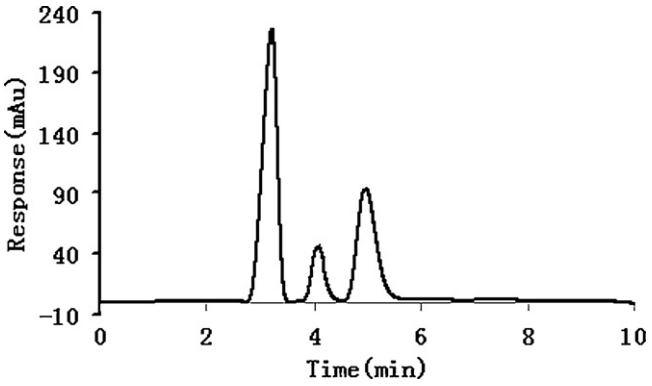

Fig. 11. Chromatograms on the APEPMOs-3 column. Mobile phase: CH_3CN:C_2H_5OH:3% TEA (pH 11.8) = 80:10:10, 220 nm, 1.0 mL/min. Peaks from left to right: metronidazole, fluconazole, isonicotinic acid.

similar alkaloids, like matrine and oxymatrine, sophocarpine and *N*-oxysophocarpine, could realize good separation on APEPMOs-3 column (Fig. 12) using low pH mobile phase (pH 1.6). Because of large specific area, there are more potential points distributed in the silica channel and surface, which is the main reason for the broad peaks. The higher chemical stability makes would endow the APEPMOs-3 material with wider pH range, thus it may have potential to satisfy more rigorous needs in chromatographic analysis. The order of peaks is the same as the commercial NH_2 column in all separations. The separating mechanism is similar with the NH_2 column, and the large-amount $-CH_2CH_2-$ groups (~6.4 mmol/g) contributed stronger retention.

The chemical stability of APEPMOs-3 was investigated using an accelerated column aging experiment by exposing the column to a 50 mM TEA (pH 10.0, 2.0 mL/min) mobile phase. For comparison, the stability of the commercial NH_2 column (Lichrospher) was investigated under identical conditions. Plots of the normalized retention factor versus time (columns were exposed to 50 mM TEA mobile phase) from accelerated aging test are shown in Fig. 13. For the commercial NH_2 column, the retention factor is maintained above 90% for the first 10 h and then decreases by 25% in the following 20 h. After 40 h washing, the column efficiency drops to 50% of the original one. The decrease of the column efficiency is due to the dissolution of silica particles and collision of silica-based framework in the highly basic medium. The APEPMOs-3 column has the similar curve during the first 10 h, and over 90% of the original column efficiency was observed. After being exposed to the TEA solution for 40 h, although a little reduction, it remains the level of 80% of the original column efficiency. The test finished at the 60th hour, and the as-prepared column still remains 80% efficiency. This result demonstrates the higher chemical stability of APEPMOs-3 in basic medium. This property can be ascribed to the base-resistance of the ethane-bridged mesoporous matrix [17,20].

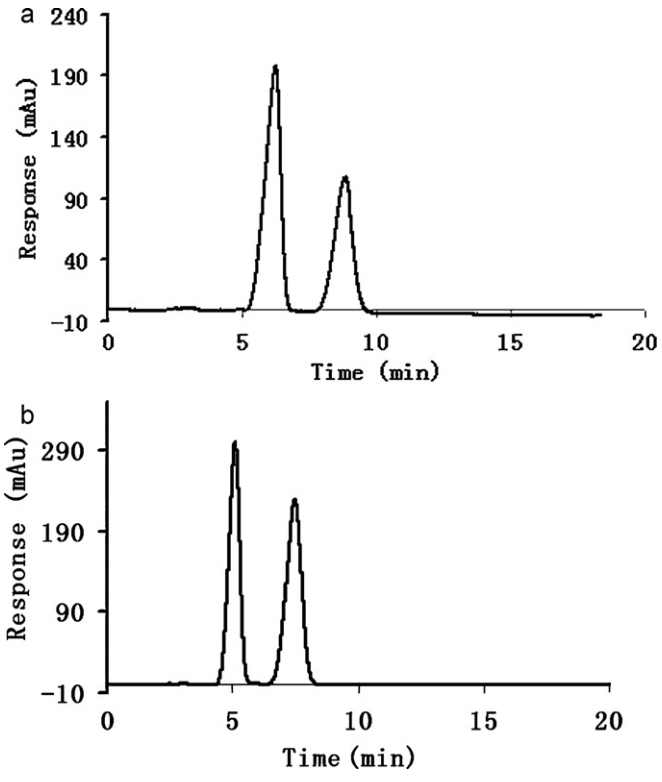

Fig. 12. Chromatograms on the APEPMOs-3 column. Mobile phase: CH_3CN:C_2H_5OH:3% H_3PO_4 (pH 1.6) = 80:10:10, 220 nm, 1.0 mL/min. (a) Peaks from left to right: matrine, oxymatrine. (b) Peaks from left to right: sophocarpine, *N*-oxysophocarpine.

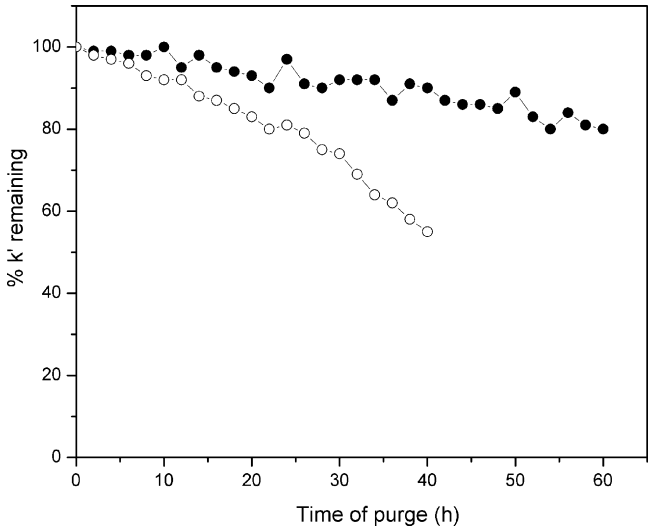

Fig. 13. Loss of the retention factor of anthracene on the APEPMOs-3 (close circle) and NH_2 (open circle) columns as a function of the purge time of 50 mM TEA solution. The test conditions are described in Section 2.4.2.

4. Conclusions

The synthesis of aminopropyl-functionalized ethane-bridged periodic mesoporous organosilicas with spherical morphology and ordered mesostructures was reported for the first time. This mesoporous material was synthesized by one-step co-condensation of BTSE and APTES with the surfactant C_{18}TACl and the co-solvent methanol in basic medium. It was found that methanol played an important role in the formation of spherical morphology. The particle size could be adjusted by varying the aging temperature and aging time. The synthesized material exhibited good mechanical and chemical stability. The chromatographic separations demonstrate that it has similar separating mechanism with the NH_2 column, and had good performance on extremely high or low pH mobile phase. These properties support APEPMOs as promising stationary phases for LC columns.

Acknowledgements

This work was financially supported by the Natural Science Foundation of Jiangsu Province of China (No. BK2009301), the Science and Technology Development Project of Changzhou City

(CS20090001) and the National Natural Science Foundation of China (21005009).

References

[1] S. Inagaki, S. Guan, Y. Fukushima, T. Ohsuna, O. Terasaki, J. Am. Chem. Soc. 121 (1999) 9611.
[2] B.J. Melde, B.T. Holland, C.F. Blanford, A. Stein, Chem. Mater. 11 (1999) 3302.
[3] T. Asefa, M.J. MacLachlan, N. Coombos, G.A. O'zin, Nature 402 (1999) 5.
[4] F. Hoffmann, M. Cornelius, J. Morell, M. Fröba, Angew. Chem. Int. Ed. 45 (2006) 3216.
[5] L. Zhang, J. Liu, J. Yang, Q.H. Yang, C. Li, Micropor. Mesopor. Mater. 109 (2008) 172.
[6] A. Calvo, M. Joselevich, G.J.A.A. Soler-Illia, F.J. Williams, Micropor. Mesopor. Mater. 121 (2009) 67.
[7] H. Yang, R. Xu, X. Xue, F. Li, G. Li, J. Hazard. Mater. 152 (2008) 690.
[8] X. Liu, Y. Du, Z. Guo, S. Gunasekaran, C.B. Ching, Y. Chen, S.S.J. Leong, Y. Yang, Micropor. Mesopor. Mater. 122 (2009) 114.
[9] V. Rebbin, M. Jakubowski, S. Pötz, M. Fröba, Micropor. Mesopor. Mater. 72 (2004) 99.
[10] D.J. Kim, J.S. Chung, W.S. Ahn, G.W. Kang, W.J. Cheong, Chem. Lett. 33 (2004) 422.
[11] V. Rebbin, M. Jakubowski, S. Pötz, M. Fröba, Stud. Surf. Sci. Catal. 154 (2004) 568.
[12] J.S. Chung, D.J. Kim, W.S. Ahn, J.H. Ko, W.J. Cheong, Korean J. Chem. Eng. 21 (2004) 132.
[13] S.S. Yoon, W.J. Son, K. Biswas, W.S. Ahn, Bull. Korean Chem. Soc. 29 (2008) 609.
[14] M.P. Kapoor, S. Inagaki, Chem. Lett. 33 (2004) 88.
[15] V. Rebbin, R. Schmidt, M. Froba, Angew. Chem. Int. Ed. 45 (2006) 5210.
[16] Y.P. Zhang, Y. Jin, H. Yu, P.C. Dai, Y.X. Ke, X.M. Liang, Talanta 81 (2010) 824.
[17] G.R. Zhu, Q.H. Yang, D.M. Jiang, J. Yang, L. Zhang, Y. Li, C. Li, J. Chromatogr. A 1103 (2006) 257.
[18] G.R. Zhu, D.M. Jiang, Q.H. Yang, J. Yang, C. Li, J. Chromatogr. A 1149 (2007) 219.
[19] G.R. Zhu, H. Zhong, Q.H. Yang, C. Li, Micropor. Mesopor. Mater. 116 (2008) 36.
[20] K.D. Wyndham, J.E. O'Gara, T.H. Walter, K.H. Glose, N.L. Lawrence, B.A. Alden, G.S. Izzo, C.J. Hudalla, P.C. Iraneta, Anal. Chem. 75 (2003) 6781.
[21] M.P. Kapoor, S. Inagaki, Chem. Mater. 14 (2002) 3509.
[22] D. Zhao, J. Feng, Q. Huo, N. Melosh, G.H. Fredrickson, B.F. Chmelka, G.D. Stucky, Science 279 (1998) 548.
[23] S. Sae-Ung, V. Boonamnuayvitaya, Environ. Eng. Sci. 25 (2008) 1477.
[24] H. Minakuchi, K. Nakanishi, N. Soga, N. Ishizuka, N. Tanaka, J. Chromatogr. A 797 (1998) 121.